An Efficient Method for Mapping High-Resolution Global River Discharge Based on the Algorithms of Drainage Network Extraction

Jiaye Li [1], Tiejian Li [1,2] (ID)**, Suning Liu [3] and Haiyun Shi [2,3,*]** (ID)

[1] State Key Laboratory of Hydroscience and Engineering, Tsinghua University, Beijing 100084, China;
    lijiaye16@mails.tsinghua.edu.cn (J.L.); litiejian@tsinghua.edu.cn (T.L.)
[2] State Key Laboratory of Plateau Ecology and Agriculture, Qinghai University, Xining 810016, China
[3] Department of Civil Engineering, The University of Hong Kong, Hong Kong 999077, China;
    u3002906@connect.hku.hk
[*] Correspondence: shihaiyun_2013@tsinghua.org.cn; Tel.: +852-2859-1970

Abstract: River discharge, which represents the accumulation of surface water flowing into rivers and ultimately into the ocean or other water bodies, may have great impacts on water quality and the living organisms in rivers. However, the global knowledge of river discharge is still poor and worth exploring. This study proposes an efficient method for mapping high-resolution global river discharge based on the algorithms of drainage network extraction. Using the existing global runoff map and digital elevation model (DEM) data as inputs, this method consists of three steps. First, the pixels of the runoff map and the DEM data are resampled into the same resolution (i.e., 0.01-degree). Second, the flow direction of each pixel of the DEM data (identified by the optimal flow path method used in drainage network extraction) is determined and then applied to the corresponding pixel of the runoff map. Third, the river discharge of each pixel of the runoff map is calculated by summing the runoffs of all the pixels in the upstream of this pixel, similar to the upslope area accumulation step in drainage network extraction. Finally, a 0.01-degree global map of the mean annual river discharge is obtained. Moreover, a 0.5-degree global map of the mean annual river discharge is produced to display the results with a more intuitive perception. Compared against the existing global river discharge databases, the 0.01-degree map is of a generally high accuracy for the selected river basins, especially for the Amazon River basin with the lowest relative error (*RE*) of 0.3% and the Yangtze River basin within the *RE* range of ±6.0%. However, it is noted that the results of the Congo and Zambezi River basins are not satisfactory, with *RE* values over 90%, and it is inferred that there may be some accuracy problems with the runoff map in these river basins.

Keywords: global river discharge; high resolution; drainage network extraction; DEM

1. Introduction

The hydrological regime of rivers is of great importance for social and economic development, such as in references [1–3]. River discharge, which represents the accumulation of surface water flowing into rivers and ultimately into the ocean or other water bodies, is one of the most important components in the global water cycle and can be essential to water availability and consequently human lives [1,4], such as in water resources management [5–7], hydropower generation [3], flood control [2], and fisheries [8]. For many of the major rivers around the world, river discharge recorded at gauging stations is regarded as an integrated signal of hydrological processes in the upstream of the corresponding gauging stations, which can provide reliable hydrological information with high

accuracy [4,9–11]. However, the global knowledge of river discharge is still poor; see references [12–14]. On the one hand, the distributed networks of gauging stations are sparse, especially in less developed countries; on the other hand, river discharge measurements are usually proprietary in many countries and cannot be shared to the public [14]. Until recently, satellite observations, which can provide spatially dense coverage and characterize river discharge variation similar to that performed at gauging stations, have been applied for mapping global river discharge; see [4,14–16].

Normally, the global river discharge databases can be obtained from the river discharge data at gauging stations worldwide, e.g., the RivDIS v1.0 database containing 949 gauging stations [17] and the RivDis2.0 database containing 3681 gauging stations, available from http://nelson.wisc.edu/. Moreover, a global map of annual river discharge, which was computed as the accumulated annual runoff along a digital drainage network with the spatial resolution of 0.5 degrees [18,19], was produced by Digital Water Altas, an activity of the Global Water System Project [20]. It is worth noting that river discharge data with such a low resolution may only be applicable to studies on the large-scale river basins, which indicates that mapping global river discharge with higher resolution is important and necessary. However, the increase of resolution may lead to serious problems of computational efficiency and accuracy [21,22]. Therefore, it is still a challenging task to develop an efficient method for mapping high-resolution global river discharge.

This study aims to develop such a method based on the algorithms of drainage network extraction proposed by Bai et al. [22]. In their study, an efficient and comprehensive method for drainage network extraction from the digital elevation model (denoted as DEM hereafter) data with billions of pixels using a size-balanced binary search tree was developed [23], and the results indicated that the developed method can be used to extract the high-resolution global drainage networks with high efficiency. Following the concepts of drainage network extraction method (i.e., including the steps of resolution matching, flow direction determination and upstream flow accumulation), an efficient method for mapping high-resolution global river discharge is proposed. In this study, a global map of mean annual runoff with the resolution of 0.5 degrees [10] is used as the input, and it is firstly downscaled to match the spatial resolution of the DEM data. Then, a global map of mean annual river discharge with the high resolution of 0.01 degrees is obtained, which is computed as the accumulated mean annual runoff along the global digital drainage networks with the same resolution (see Section 3.1 for details). Finally, the results are quantitatively evaluated through comparing against the existing global river discharge databases (see Section 3.2 for details). Overall, the proposed method will be valuable for making better decisions on water-related issues such as flood control, integrated water resources management, and ecological environment assessment.

2. Data and Methods

2.1. Global Map of Mean Annual Runoff

Spatially distributed runoff can be estimated by models with a variety of climate data such as precipitation, air temperature, radiation, vapor pressure and wind speed [24]. Combining the observed river discharge information with the outputs from the climate-driven global water balance model developed by the University of New Hampshire [25], Fekete et al. [10] proposed a global map of mean annual runoff with a spatial resolution of 0.5 degrees (see Figure 1). This map was produced based on the assumption that the mean annual discharge difference between a station and its upstream neighbor represents the mean annual runoff generated in the interstation region. Selected 663 gauging stations from the World Meteorological Organization Global Runoff Data Centre were geographically co-registered to a 0.5-degree grid-based simulated topological network (STN-30p) [18], and interstation regions between gauging stations along the STN-30p network were identified. Then, the mean annual runoff of an interstation region was calculated by multiplying a correction factor which is equal to the ratio of observed and simulated long-term mean discharge during 1950–2000 [26]. This map is of great

importance to water-related fields, such as terrestrial modeling, climate-atmosphere interactions, and global water resource assessments, e.g., [27–31].

In this study, this map is introduced and used as the primary input to map high-resolution global river discharge. Considering its relatively low spatial resolution, spatial downscaling, which can separate an original pixel into a number of smaller sub-pixels, is necessary [32]. Moreover, several studies [33–35] revealed that the spatial resolution of 1 km (~0.01-degree) would be suitable for hydrological simulation, and therefore, this study selected this resolution for the global river discharge map. Subsequently, each original pixel of the global mean annual runoff map is separated into 2500 (=50 × 50) smaller sub-pixels.
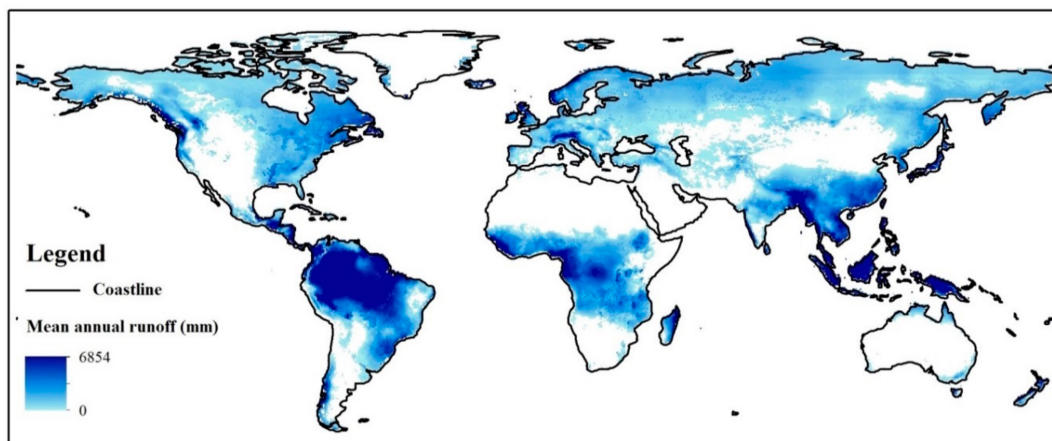

Figure 1. A global map of mean annual runoff during the period 1950–2000 with a spatial resolution of 0.5 degrees [10].

2.2. Mapping High-Resolution Global River Discharge

In order to calculate river discharge using the runoff map as the input, the major steps are flow direction determination and upstream flow accumulation, which can be derived from the algorithms of drainage network extraction. It is worth noting that high-resolution DEM data are also introduced because of its vital role in drainage network extraction. In this study, the Advanced Spaceborne Thermal Emission and Reflection Radiometer (ASTER) Global DEM dataset [36] with 1-arc-second resolution (approximately 30 m) is used. Due to the different spatial resolutions of the runoff map and the DEM data, the pretreatment process named resolution matching is necessary. Figure 2 shows the framework diagram of the mapping method, and the details are introduced as follows.

2.2.1. Resolution Matching

The original pixel size of the global mean annual runoff map is 0.5-degree (see Figure 2b), while the original pixel size of the ASTER Global DEM dataset is 1-arc-second (see Figure 2a). As mentioned in Section 2.1, the resolution of the global mean annual runoff map will be downscaled into 0.01-degree (see Figure 2d). Therefore, the original pixels of the ASTER Global DEM dataset are aggregated to pixels with the same resolution (see Figure 2c). Such a procedure can be completed using the majority resampling method integrated the ArcGIS software. After this resolution matching, each pixel of the downscaled global mean annual runoff map can correspond to a unique pixel of the upscaled ASTER Global DEM dataset with the same geographical coordinates, which is the basis of subsequent steps.

2.2.2. Flow Direction Determination

To assign the flow direction, it is of great importance to know the topological relationships of a designated pixel with its neighboring pixels; e.g., if the two pixels regarded as upstream and downstream, respectively. We cannot achieve this if we use the global mean annual runoff map

only. However, flow direction can be easily determined with the DEM data using different methods, e.g., [37–39]. That is why we introduce the ASTER Global DEM dataset in this study and match its resolution with that of the global mean annual runoff map (see Figure 2e). For convenience, two layers, which denote the downscaled global mean annual runoff map (Layer I) and the upscaled ASTER Global DEM dataset (Layer II), respectively, are defined in this study. For a designated pixel in Layer I, the flow direction can be determined as follows: first, to find the unique pixel in Layer II corresponding to the designated pixel in Layer I. Second, to determine the flow direction of this corresponding pixel in Layer II based on the method for drainage network extraction from the DEM data [22], i.e., the two pixels regarded as the upstream and downstream of this corresponding pixel in Layer II. Third, to find the two corresponding pixels in Layer I, which are the upstream and downstream of the designated pixel in Layer I.
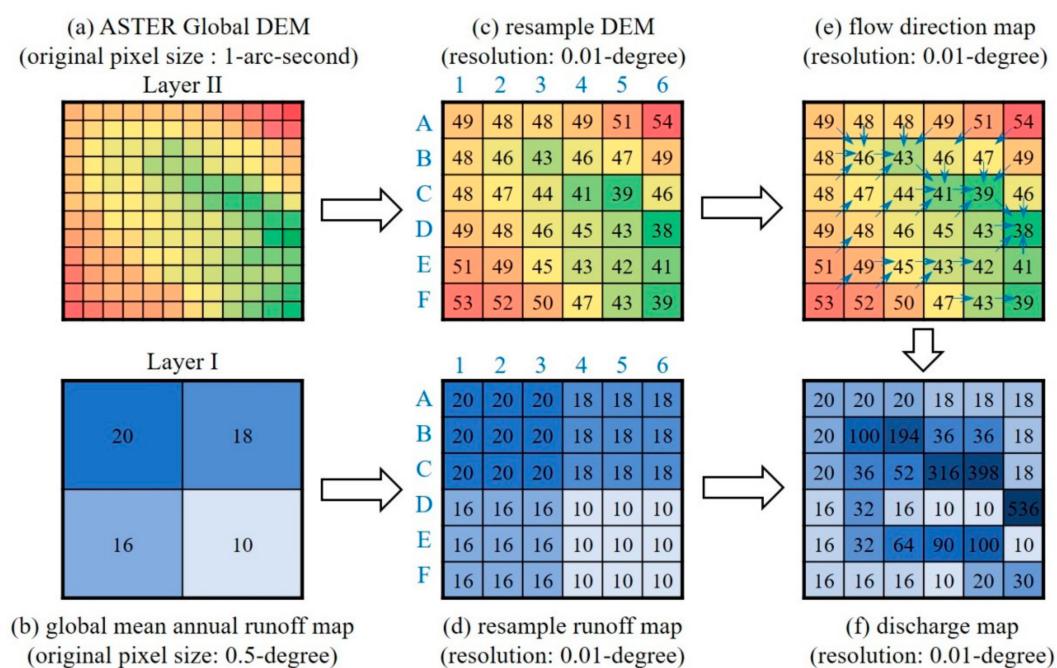

Figure 2. A framework diagram of the mapping method. ASTER: Advanced Spaceborne Thermal Emission and Reflection Radiometer; DEM: digital elevation model.

According to the study of Bai et al. [22], the flow direction of a pixel in Layer II can be determined by finding the optimal flow path among its eight directions (i.e., east, southeast, south, southwest, west, northwest, north and northeast), through which the interior pixel can flow to the outlet pixels in the shortest routing distances. In comparison with the commonly used D8 method which depends on local topographic slopes, the optimal flow path method based on the sorted pixel sequence has an advantage in terms of the flow direction determination in a flat area [22] because the local slopes may be the same in a flat area and they might lead to nested loops of flow directions. Moreover, the optimal flow path method is simpler and faster than the traditional D8 method for practical operations.

2.2.3. Upstream Flow Accumulation

The objective of this step is to calculate the river discharge for the designated pixel in Layer I through summing the runoffs of all the pixels upstream of this pixel. Similar to that in the last step, the unique pixel in Layer II corresponding to the designated pixel in Layer I is found first. Second, the upstream pixels are identified in Layer II because this can be achieved by tracing the flow directions from the most upslope pixels [22,39,40], i.e., the upslope area accumulation step in the study of Bai et al. [22]. Then, the corresponding upstream pixels are found in Layer I. Finally, the runoffs of

these pixels are accumulated to generate the river discharge for the designated pixel in Layer I (see Figure 2f).

According to the study of Bai et al. [22], the upslope area accumulation is as follows. First, the upslope area of each pixel is initially assigned its unit size. The upslope area accumulation then loops from the pixel in the tail of the sorted sequence with the maximum elevation to the pixel in the head with the minimum elevation. In each loop, the upslope area of the current pixel contributes to that of its downslope pixel. Finally, all upslope areas are accumulated until the outlet pixels are contributed. Because the upslope area accumulation for each pixel can be guaranteed from the upslope to the downslope, the efficiency of the upslope area accumulation can be significantly improved with a calculation loop based on the sorted pixel sequence. This is particularly valuable for mapping the global river discharge at a high resolution because there may be a mass of pixels (e.g., billions of pixels) need to be processed in such case.

2.3. Assessment Criteria

In order to quantitatively evaluate the performance of the obtained global river discharge map, the following objective function is used as assessment criteria, namely relative error (*RE*). The equation to compute the *RE* value is given as follows:

$$RE = (Q_{com} - Q_{exi})/Q_{exi} \tag{1}$$

where Q_{com} is the computed river discharge value of this study, and Q_{exi} is the river discharge value derived from the existing global river discharge databases at the same location.

In addition, the performance of the obtained global river discharge map will be evaluated using the Taylor Diagram, which can summarize multiple aspects of the model performance (i.e., correlation, root-mean-square error, and standard deviation) in a single diagram [41].

3. Results and Discussion

3.1. Map of Global River Discharge

Using the proposed mapping method, a global map of mean annual river discharge with a spatial resolution of 0.01 degrees is obtained (see Figure 3a). This map is produced based on the algorithms of drainage network extraction, and thus the river discharge values will appear along the drainage networks, and the drainage networks with the higher Strahler stream orders [42,43] will have a darker blue color, which indicates larger river discharge values. Unfortunately, due to the small pixel size (i.e., 0.01 degrees), the pixels with the darker blue color are generally surrounded by a mass of pixels with the lighter blue color, resulting in the global map seeming unlikely to be well displayed in a single figure when setting the spatial resolution as that suitable for printing (e.g., 300 or 600 dpi). Only a number of separated points with a darker blue color can be observed in the global map of Figure 3a. However, when zooming in and focusing on different river basins, the relevant results can be well displayed at the regional scale. In Figure 3a, the Congo River basin in Africa is selected as an example to display the results. It is observed that the river discharge values appear along the drainage networks and the larger river discharge values can be found in stream channels with the higher Strahler stream orders.

In order to display the results with a more intuitive perception, a global map of the mean annual river discharge with the spatial resolution of 0.5-degree is also obtained through a resampling procedure (see Figure 3b). It is worth noting that each pixel with the spatial resolution of 0.5-degree will cover 2500 (=50 × 50) pixels with the spatial resolution of 0.01-degree. Therefore, the maximum river discharge value among those of all the 2500 0.01-degree pixels covered by the corresponding 0.5-degree pixel is assigned to the corresponding 0.5-degree pixel during this procedure in this study (see Figure 4). It is worth noting that, inevitably, lots of information will be lost during this procedure, and only the discharges of the main streams which we most care about are retained. As mentioned above,

Global Water System Project (GWSP) Digital Water Atlas [20] also produced a global map of annual river discharge with a spatial resolution of 0.5 degrees. Through comparing the results shown in Figure 3b against those produced by GWSP Digital Water Atlas [20], it is found that the colored parts and the distribution patterns of the river discharge values in these two maps are basically the same. However, the map in this study can show the stream channels more clearly than that produced by GWSP Digital Water Atlas [20]. This is mainly because the map in this study is from the 0.01-degree-resolution global drainage network extracted from the 30-m-resolution DEM data [22,44], which has the much higher spatial resolution than that (i.e., 0.5-degree) used by GWSP Digital Water Atlas [20].
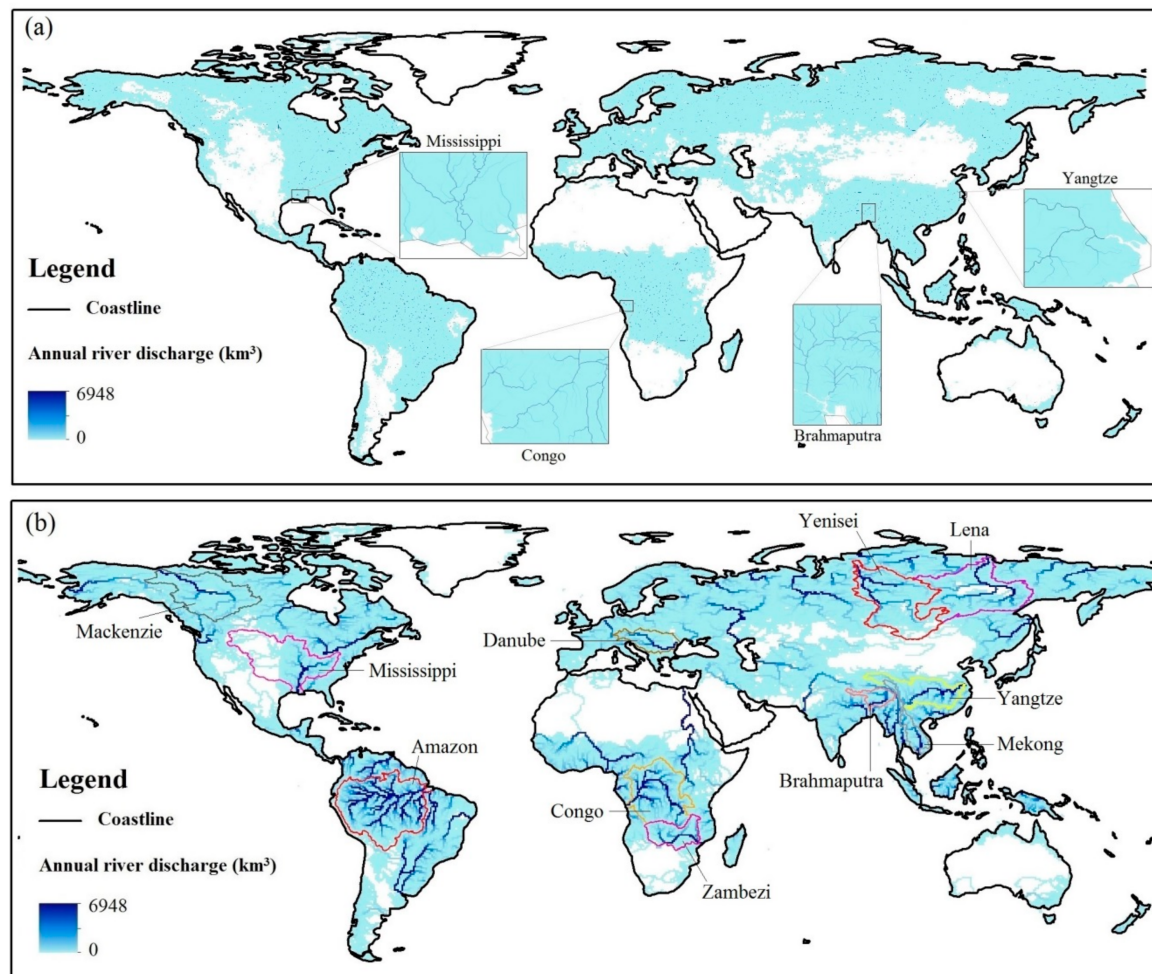

Figure 3. The global maps of the mean annual river discharge with spatial resolutions of (**a**) 0.01 degrees and (**b**) 0.5 degrees, respectively.
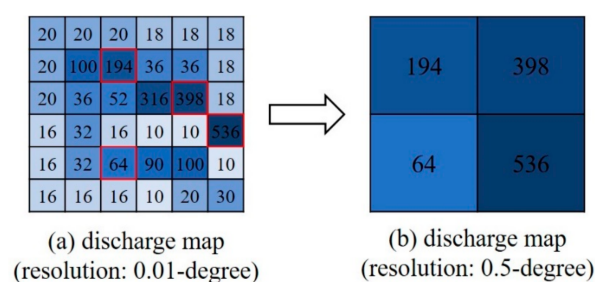

Figure 4. The procedure for resampling the spatial resolution of the global river discharge map from (**a**) 0.01 degrees to (**b**) 0.5 degrees.

In addition, by comparing Figures 1 and 3b, it is found that the distributions of the colored parts in these two maps have overall similar characteristics; however, more colored regions shaped as stream channels can be observed in Figure 3b (e.g., central Asia, northern and southern Africa, central North America, and southern South America). The reason for this is as follows: there may be no local runoff or the runoff data may be missing in those regions (i.e., blank in Figure 1); however, due to the flow concentration processes, there will be river discharges in the stream channels which are generated from runoff in the upstream regions. Therefore, such influence cannot be ignored in the above-mentioned regions.

3.2. Accuracy Evaluation

To quantitatively evaluate the accuracy of the global map of the mean annual river discharge with a spatial resolution of 0.01 degrees, the river discharge values are compared against those recorded in the existing global river discharge databases, and 11 river basins (i.e., Yangtze, Mekong, Brahmaputra, Yenisei and Lena River basins in Asia, Mississippi and Mackenzie River basins in North America, Amazon River basin in South America, Danube River basin in Europe, and Congo and Zambezi River basins in Africa) are selected as examples (Table 1). The locations of these 11 river basins are shown in Figure 3b.

In this study, the RivDis2.0 database is selected as the representative of the existing global river discharge databases. It is worth noting that some of the mean annual river discharge values recorded in this database are not measured at the river mouths. For example, the mean annual river discharge of the Amazon River basin in the RivDis2.0 database is the value recorded at the Obidos station, the controlled basin area of which is only 4.62 million km^2 and much smaller than the total basin area of Amazon River basin (i.e., 6.915 million km^2). The same problem also exists in Yangtze, Mekong, Mackenzie and Zambezi River basins, which may lead to the large *RE* values when comparing with the results obtained in this study. Therefore, additional references would be necessary. Wohl [45] has reported the basic hydrological characteristics (including annual river discharge) of the world's major river basins, which are considered as the other reference in this study. The annual river discharge values of the eleven river basins derived from these two data sources are listed in Table 1. It is observed that the annual river discharge values from the two data sources are similar in Brahmaputra, Mississippi, Lena, Congo and Zambezi River basins, while the annual river discharge values from the RivDis2.0 database are much lower than those from the study of Wohl [45] in Amazon, Yangtze, Mekong, Danube, Yenisei and Mackenzie River basins.

Table 1. Comparison of the annual river discharge values in this study and the existing global river discharge databases for the world's major river basins.

River Basin	Annual River Discharge (km^3)			*RE* (%)	
	Wohl (2007)	RivDis2.0	This Study	Wohl (2007)	RivDis2.0
Amazon	**6930**	**5414** [1]	**6948**	**0.3**	**28.3**
Yangtze	**870**	**789** [2]	**826**	**−5.1**	**4.7**
Mekong	**667**	**252** [3]	**720**	**7.9**	**185.7**
Danube	**282**	**205**	**222**	**−21.3**	**8.3**
Brahmaputra	612.5	620	540	−11.7	−12.7
Mississippi	562	537	486	−13.5	−9.5
Yenisei	620	558	390	−37.1	−30.1
Lena	525	524	308	−41.3	−41.2
Mackenzie	306	263 [4]	168	−45.1	−36.1
Congo	*1250*	*1264*	*2488*	*99.0*	*96.8*
Zambezi	*106*	*105* [5]	*350*	*230.2*	*233.3*

[1] This is the value recorded at the Obidos station, the controlled basin area of which is 4.62 million km^2. [2] This is the value recorded at the Datong station, the controlled basin area of which is 1.70 million km^2. [3] This is the value recorded at the Mukdahan station, the controlled basin area of which is 0.39 million km^2. [4] This is the value recorded at the NormanWells station, the controlled basin area of which is 1.57 million km^2. [5] This is the value recorded at the Matundo–Cais station, the controlled basin area of which is 0.94 million km^2.

Furthermore, the annual river discharge values derived from the proposed method in this study are also listed in Table 1, and the corresponding *RE* values are computed using Equation (1). When comparing against the annual river discharge values from the study of Wohl [45], the *RE* values vary greatly, with the lowest value of 0.3% in the Amazon River basin and the highest value of 230.2% in the Zambezi River basin, respectively. By contrast, the *RE* values vary from 4.7% (Yangtze River basin) to 233.3% (Zambezi River basin) when comparing against the annual river discharge values from the RivDis2.0 database. Specifically, according to the performances of the obtained annual river discharge values in different river basins, the comparison results can be divided into the following three categories:

(1) The obtained annual river discharge values are very close to those in at least one of the two existing global river discharge databases, e.g., in the Amazon, Yangtze, Mekong and Danube River basins (see the river basins in bold format in Table 1). In particular, when comparing against the annual river discharge values from the study of Wohl [45], the *RE* values are only 0.3% for the Amazon River basin and −5.1% for the Yangtze River basin, respectively. Moreover, even if the mean annual river discharges of these two river basins in the RivDis2.0 database are not measured at the river mouths, the *RE* values are only 28.3% for the Amazon River basin and 4.7% for the Yangtze River basin. It is observed from Figure 1 that the runoff data within these two river basins are complete, and therefore the feasibility and accuracy of this mapping method can be proved. In addition, low *RE* values are obtained for the Mekong River basin (i.e., 7.9% when comparing against the annual river discharge values from the study of Wohl [45]) and the Danube River basin (i.e., 8.3% when comparing against the annual river discharge values from the RivDis2.0 database), respectively.

(2) The obtained annual river discharge values are generally smaller than those in the existing global river discharge databases, e.g., in Brahmaputra, Mississippi, Yenisei, Lena and Mackenzie River basins (see Table 1). When comparing against the annual river discharge values from the study of Wohl [45], the *RE* values are between −11.7% and −45.1%; in contrast, when comparing against the annual river discharge values in the RivDis2.0 database, the *RE* values are between −9.5% and −41.2%. The reason for such biases is as follows: known from Figure 1, there are blank pixels within the Mississippi, Yenisei, Lena and Mackenzie River basins, which may indicate that the runoff data are incomplete in those pixels. The data missing problem can lead to the underestimation of river discharge values. However, within the Brahmaputra River basin, the runoff data are complete (see Figure 1), so the underestimation of river discharge value may be caused by the accuracy of the runoff data. A part of this river basin is located in the Tibetan Plateau, a mountainous region with significant topographic variation, which may lead to the difficulty in measuring meteorological and hydrological data (e.g., sparse stations) [46].

(3) The obtained annual river discharge values are significantly larger than those in the existing global river discharge databases, e.g., in the Congo and Zambezi River basins (see the river basins in italic format in Table 1). Although the runoff data are basically complete in these two river basins (see Figure 1), the accuracy of the data is still worth further study due to limited data availability in Africa [47]. Figure 5 shows the original runoff maps of Congo (left) and Zambezi (right) River basins. For the Congo River basin, the mean runoff is about 651 mm and the basin area is 3.82 million km^2, and thus the total annual discharge is about 2488 km^3, which is the same as the value listed in Table 1. For the Zambezi River basin, the mean runoff is about 263 mm and the basin area is 1.33 million km^2, and thus, the total annual discharge is about 350 km^3, which is also the same as the value listed in Table 1. Moreover, as the feasibility and accuracy of this mapping method has been proved in the Amazon and Yangtze River basins, where the data quality is considered to be good, it is inferred that there may be some accuracy problems with the original runoff maps in Congo and Zambezi River basins.

In addition, the Taylor diagram [41] is adopted in this study to further evaluate the performance of the obtained global river discharge map (Figure 6). It is clear that the annual river discharge values from this study (i.e., represented by the black points in Figure 6) are closer to those from the study

of Wohl [45] (i.e., represented by the blue points in Figure 6) rather than those from the RivDis2.0 database (i.e., represented by the red points in Figure 6). Moreover, the performance can be much better if excluding the results of the Congo and Zambezi River basins. As the coefficients of correlation are both high (i.e., >0.99) and the root mean square errors are both small (i.e., <0.25) in Figure 6b, the obtained global river discharge map can be regarded to be highly accurate.
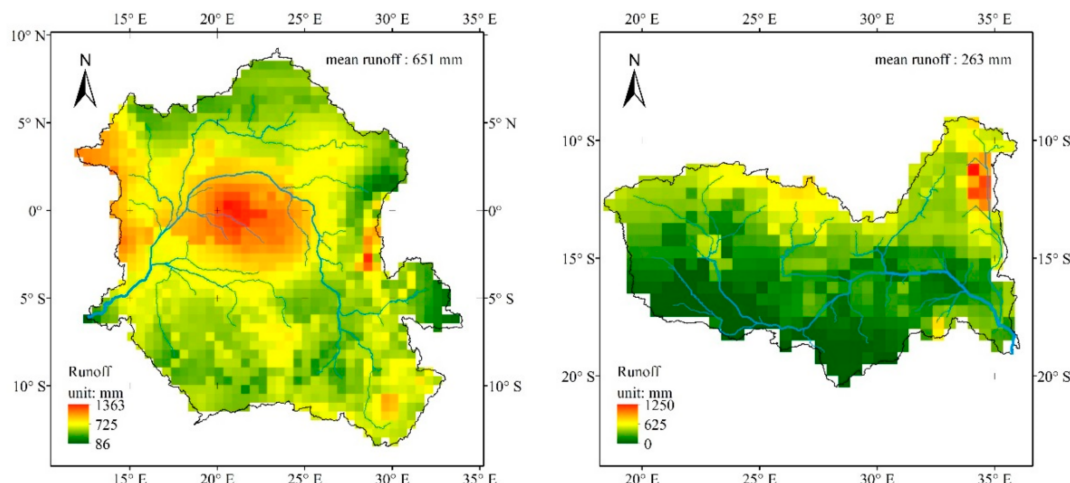

Figure 5. The original runoff maps of the Congo (**left**) and Zambezi (**right**) River basins.
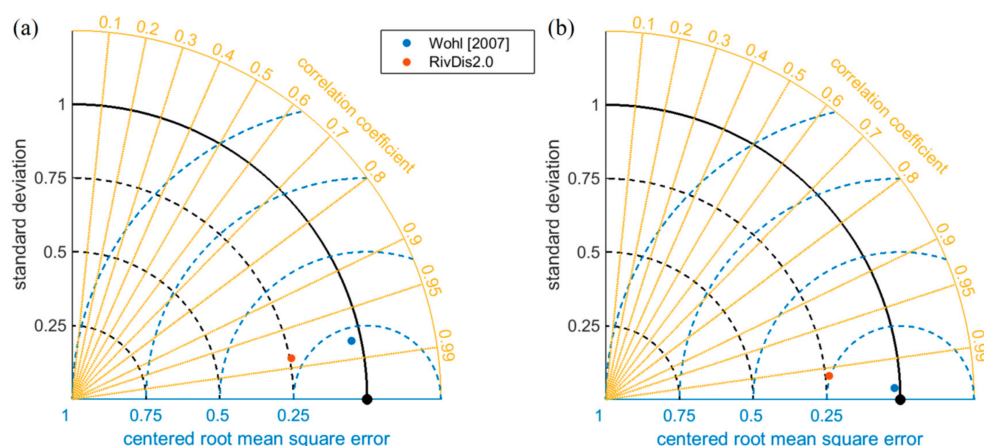

Figure 6. The normalized Taylor diagrams displaying the differences between the annual river discharge values from this study and the existing global river discharge databases for (**a**) eleven river basins and (**b**) nine river basins excluding Congo and Zambezi River basins.

3.3. Discussion

To the best of our knowledge, there have only recently been a few studies [48,49] focusing on mapping high-resolution global river discharge. Barbarossa et al. [48] have developed a global-scale regression model to quantify the mean annual discharge based on the observations of discharge and river basin characteristics from 1885 river basins worldwide, and this model can be applied globally to estimate the mean annual discharge at any point of the river network. Moreover, Barbarossa et al. [49] have created FLO1K, a consistent discharge dataset at a resolution of 30 arc seconds (~1 km) and global coverage, by means of artificial neural networks regression using the observations of discharge from 6600 monitoring stations worldwide. By contrast, this study has provided another way of mapping high-resolution global river discharge: first, the map has been produced based on the algorithms of drainage network extraction rather than regression methods. Second, the input data are the grid-based

data rather than the observations from monitoring stations. It is worth noting that the spatial resolution (i.e., 0.01-degree, 36 arc seconds) of the global river discharge map in this study is close to that in the study of Barbarossa et al. [49]. However, only the global map of the mean annual river discharge has been produced in this study, while Barbarossa et al. [49] have produced the global maps of the mean, maximum and minimum annual river discharge for each year in the period 1960–2015.

Nevertheless, the proposed method and obtained results in this study will be of great value to water-related studies. Applying the proposed method for mapping high-resolution global river discharge, we also need to be fully aware of the limitations of this study, which are mainly related to the following four aspects. First, the spatial resolution of the primary input (i.e., the 0.5-degree global mean annual runoff map) is not high, and the downscaling process of this map will inevitably bring in errors. Moreover, further studies may be necessary to ensure the data integrity and accuracy in some river basins (e.g., Mississippi, Yenisei, Lena and Mackenzie River basins in this study). If the more complete and accurate runoff data with higher spatial resolution can be made available, it is believed that the accuracy of the global river discharge map will be higher. Second, limited by the fact that only the mean annual river discharge values in the world's major river basins have been provided in the study of Wohl [45], only the obtained results of eleven major river basins around the world are quantitatively validated in this study. Although the accuracy is generally high, the obtained results should be further validated in more river basins, especially for smaller river basins. Third, at this stage, this study only compares the results at the river mouths of several major river basins. If more observed data recorded at some representative stations within the river basins can be made available, the accuracy of the proposed method can be further evaluated. Fourth, the existing global river discharge values from two data sources are used as reference values in this study, and the relevant results are basically satisfactory; however, more existing databases can be adopted to perform more comprehensive validations in future work.

Furthermore, the method proposed in this study will be more practical if the inputs can be the global precipitation and actual evapotranspiration data. On the one hand, these two types of data are easier to obtain. Global precipitation data, e.g., the Climate Prediction Center morphing method (CMORPH) dataset and Tropical Rainfall Measuring Mission (TRMM) multi-satellite precipitation analysis (TMPA) dataset, can be derived primarily by merging various passive microwave observations from the low-earth orbit satellites [50,51], and the global precipitation data can be obtained based on the energy balance using the thermal satellite data [52]. On the other hand, these two types of data can be multi-source [35], which may reduce the uncertainty of the input. Since the global runoff data can be calculated from the global precipitation and actual evapotranspiration data through a variety of ways such as water balance methods [53] and hydrological models [54], it is possible to further develop a method for mapping the global river discharge using the global precipitation and actual evapotranspiration data as the inputs in future works.

4. Conclusions

This study proposes an efficient method for mapping high-resolution global river discharge based on the algorithms of drainage network extraction, and the major contributions of this study can be summarized as follows:

First, the flow direction determination (i.e., the optimal flow path method) and upstream flow accumulation (i.e., a calculation loop based on the sorted pixel sequence) algorithms used in global drainage network extraction [22] have been introduced, which can be particularly valuable for efficiently mapping the global river discharge at a very high resolution (i.e., 0.01-degree) because there may be billions of pixels need to be processed.

Second, the global maps of mean annual river discharge with two different spatial resolutions (i.e., 0.01-degree and 0.5 degree) are provided. The 0.01-degree map can be used for high-resolution studies on the water-related issues, and the 0.5-degree map is mainly used for displaying the results with a more intuitive perception.

Third, an accuracy evaluation of the 0.01-degree map has been conducted through comparing it against the existing global river discharge databases, and the results indicate that the 0.01-degree map is of generally high accuracy for most of the selected river basins. Therefore, the proposed method is feasible for mapping high-resolution global river discharge.

In addition, the results may be improved by using input with higher spatial resolution, and more comprehensive validations may be needed either through the use of more existing databases or more river basins in future works. Nevertheless, the current results would still be valuable for making better decisions on issues related to flood control, integrated water resources management, ecological environment assessment, and so on in future, e.g., [3,25,35,55–57].

Author Contributions: Haiyun Shi conceived and designed the methodology, and revised the paper; Jiaye Li developed the algorithms and wrote the paper; all the four authors contributed to the analyses of the results.

Conflicts of Interest: The authors declare no conflict of interest.

References

1. Zhou, X.Y.; Zhang, Y.Q.; Wang, Y.P.; Zhang, H.Q.; Vaze, J.; Zhang, L.; Yang, Y.H.; Zhou, Y.C. Benchmarking global land surface models against the observed mean annual runoff from 150 large basins. *J. Hydrol.* **2012**, *470–471*, 269–279. [CrossRef]

2. Van Vliet, M.T.H.; Franssen, W.H.P.; Yearsley, J.R.; Ludwig, F.; Haddeland, I.; Lettenmaier, D.P.; Kabat, P. Global river discharge and water temperature under climate change. *Glob. Environ. Chang.* **2013**, *23*, 450–464. [CrossRef]

3. Chen, J.; Shi, H.Y.; Sivakumar, B.; Peart, M.R. Population, water, food, energy and dams. *Renew. Sustain. Energy Rev.* **2016**, *56*, 18–28. [CrossRef]

4. Brakenridge, G.R.; Cohen, S.; Kettner, A.J.; De Groeve, T.; Nghiem, S.V.; Syvitski, J.P.M.; Fekete, B.M. Calibration of satellite measurements of river discharge using a global hydrology model. *J. Hydrol.* **2012**, *475*, 123–136. [CrossRef]

5. Haag, I.; Westrich, B. Processes governing river water quality identified by principal component analysis. *Hydrol. Process.* **2002**, *16*, 3113–3130. [CrossRef]

6. Aerts, J.C.J.H.; Renssen, H.; Ward, P.J.; de Moel, H.; Odada, E.; Bouwer, L.M.; Goosse, H. Sensitivity of global river discharges under Holocene and future climate conditions. *Geophys. Res. Lett.* **2006**, *33*, L19401. [CrossRef]

7. Nurnberg, D.; Ziegler, M.; Karas, C.; Tiedemann, R.; Schmidt, M.W. Interacting Loop Current variability and Mississippi River discharge over the past 400 kyr. *Earth Planet. Sci. Lett.* **2008**, *272*, 278–289. [CrossRef]

8. Ficke, A.D.; Myrick, C.A.; Hansen, L.J. Potential impacts of global climate change on freshwater fisheries. *Rev. Fish Biol. Fish.* **2007**, *17*, 581–613. [CrossRef]

9. Dingman, S.L. *Physical Hydrology*; Prentice Hall: Englewood Cliffs, NJ, USA, 2001.

10. Fekete, B.M.; Vörösmarty, C.J.; Grabs, W. High-resolution fields of global runoff combining observed river discharge and simulated water balances. *Glob. Biogeochem. Cycles* **2002**, *16*, 1042. [CrossRef]

11. Zaitchik, B.F.; Rodell, M.; Olivera, F. Evaluation of the Global Land Data Assimilation System using global river discharge data and a source-to-sink routing scheme. *Water Resour. Res.* **2010**, *46*, W06507. [CrossRef]

12. Vörösmarty, C.J.; McIntyre, P.B.; Gessner, M.O.; Dudgeon, D.; Prusevich, A.; Green, P.; Glidden, S.; Bunn, S.E.; Sullivan, C.A.; Reidy Liermann, C.; et al. Global threats to human water security and river biodiversity. *Nature* **2010**, *467*, 555–561. [CrossRef] [PubMed]

13. Hannah, D.M.; Demuth, S.; van Lanen, H.A.J.; Looser, U.; Prudhomme, C.; Rees, G.; Stahl, K.; Tallaksen, L.M. Large-scale river flow archives: Importance, current status and future needs. *Hydrol. Process.* **2011**, *25*, 1191–1200. [CrossRef]

14. Gleason, C.J.; Smith, L.C. Toward global mapping of river discharge using satellite images and at-many-stations hydraulic geometry. *Proc. Natl. Acad. Sci. USA* **2014**, *111*, 4788–4791. [CrossRef] [PubMed]

15. Syed, T.H.; Famiglietti, J.S.; Chambers, D.P.; Willis, J.K.; Hilburn, K. Satellite-based global-ocean mass balance estimates of interannual variability and emerging trends in continental freshwater discharge. *Proc. Natl. Acad. Sci. USA* **2010**, *107*, 17916–17921. [CrossRef] [PubMed]

16. Temimi, M. A multi-temporal analysis of AMSR-E data for flood and discharge monitoring during the 2008 flood in Iowa. *Hydrol. Process.* **2011**, *25*, 2623–2634. [CrossRef]

17. Vörösmarty, C.J.; Fekete, B.M.; Tucker, B.A. *Global River Discharge Database (RivDIS v1.0)*; The United Nations Educational, Scientific and Cultural Organisation (UNESCO): London, UK, 1996. Available online: http://unesdoc.unesco.org/images/0010/001051/105190Eb.pdf (accessed on 25 March 2018).

18. Vörösmarty, C.J.; Fekete, B.M.; Meybeck, M.; Lammers, R.B. Geomorphometric attributes of the global system of rivers at 30-minute spatial resolution. *J. Hydrol.* **2000**, *237*, 17–39. [CrossRef]

19. Fekete, B.M.; Vörösmarty, C.J.; Lammers, R.B. Scaling gridded river networks for macroscale hydrology: Development, analysis, and control of error. *Water Resour. Res.* **2001**, *37*, 1955–1967. [CrossRef]

20. GWSP Digital Water Atlas. *Annual River Discharge (V1.0)*; GWSP Digital Water Atlas: Bonn, Germany, 2008. Available online: http://atlas.gwsp.org (accessed on 25 March 2018).

21. Metz, M.; Mitasova, H.; Harmon, R.S. Efficient extraction of drainage networks from massive, radar-based elevation models with least cost path search. *Hydrol. Earth Syst. Sci.* **2011**, *15*, 667–678. [CrossRef]

22. Bai, R.; Li, T.J.; Huang, Y.F.; Li, J.Y.; Wang, G.Q. An efficient and comprehensive method for drainage network extraction from DEM with billions of pixels using a size-balanced binary search tree. *Geomorphology* **2015**, *238*, 56–67. [CrossRef]

23. Li, T.J.; Wang, G.Q.; Chen, J. A modified binary tree codification of drainage networks to support complex hydrological models. *Comput. Geosci.* **2010**, *36*, 1427–1435. [CrossRef]

24. Vörösmarty, C.J.; Moore, B., III; Grace, A.L.; Gildea, M.; Melillo, J.M.; Peterson, B.J.; Rastetter, E.B.; Steudler, P.A. Continental-scale models of water balance and fluvial transport: An application to South America. *Glob. Biogeochem. Cycles* **1989**, *3*, 241–265. [CrossRef]

25. Vörösmarty, C.J.; Federer, C.A.; Schloss, A.L. Potential evaporation functions compared on U.S. watersheds: Possible implications for global-scale water balance and terrestrial ecosystem modeling. *J. Hydrol.* **1998**, *207*, 147–169. [CrossRef]

26. Hunger, M.; Döll, P. Value of river discharge data for global-scale hydrological modeling. *Hydrol. Earth Syst. Sci.* **2008**, *12*, 841–861. [CrossRef]

27. Sood, A.; Smakhtin, V. Global hydrological models: A review. *Hydrol. Sci. J.* **2015**, *60*, 549–565. [CrossRef]

28. McMillan, H.K.; Booker, D.J.; Cattoën, C. Validation of a national hydrological model. *J. Hydrol.* **2016**, *541*, 800–815. [CrossRef]

29. Schumann, G.J.-P.; Stampoulis, D.; Smith, A.M.; Sampson, C.C.; Andreadis, K.M.; Neal, J.C.; Bates, P.D. Rethinking flood hazard at the global scale. *Geophys. Res. Lett.* **2016**, *43*, 10249–10256. [CrossRef]

30. Faramarzi, M.; Abbaspour, K.C.; Adamowicz, W.L.; Lu, W.; Fennell, J.; Zehnder, A.J.B.; Goss, G.G. Uncertainty based assessment of dynamic freshwater scarcity in semi-arid watersheds of Alberta, Canada. *J. Hydrol. Reg. Stud.* **2017**, *9*, 48–68. [CrossRef]

31. Yang, H.; Zhou, F.; Piao, S.; Huang, M.; Chen, A.; Ciais, P.; Li, Y.; Lian, X.; Peng, S.; Zeng, Z. Regional patterns of future runoff changes from Earth system models constrained by observation. *Geophys. Res. Lett.* **2017**, *44*, 5540–5549. [CrossRef]

32. Mehrotra, R.; Evans, J.P.; Sharma, A.; Sivakumar, B. Evaluation of downscaled daily rainfall hindcasts over Sydney, Australia using statistical and dynamical downscaling approaches. *Hydrol. Res.* **2014**, *45*, 226–249. [CrossRef]

33. Sangati, M.; Borga, M. Influence of rainfall spatial resolution on flash flood modelling. *Nat. Hazards Earth Syst. Sci.* **2009**, *9*, 575–584. [CrossRef]

34. Lobligeois, F.; Andreassian, V.; Perrin, C.; Tabary, P.; Loumagne, C. When does higher spatial resolution rainfall information improve streamflow simulation? An evaluation using 3620 flood events. *Hydrol. Earth Syst. Sci.* **2014**, *18*, 575–594. [CrossRef]

35. Shi, H.Y.; Chen, J.; Li, T.J.; Wang, G.Q. A new method for estimation of spatially distributed rainfall through merging satellite observations, raingauge records, and terrain digital elevation model data. *J. Hydro-Environ. Res.* **2017**. [CrossRef]

36. ASTER GDEM Validation Team. *ASTER Global DEM Version 2–Summary of Validation Results*; Ministry of Economy, Trade, and Industry (METI): Tokyo, Japan; United States National Aeronautics and Space Administration (NASA): Washington, DC, USA, 2011.

37. Holmgren, P. Multiple flow direction algorithms for runoff modelling in grid based elevation models: An empirical evaluation. *Hydrol. Process.* **1994**, *8*, 327–334. [CrossRef]

38. Wolock, D.M.; McCabe, G.J. Comparison of single and multiple flow direction algorithms for computing topographic parameters in TOPMODEL. *Water Resour. Res.* **1995**, *31*, 1315–1324. [CrossRef]

39. Garbrecht, J.; Martz, L.W. The assignment of drainage direction over flat surfaces in raster digital elevation models. *J. Hydrol.* **1997**, *193*, 204–213. [CrossRef]

40. Choi, Y. A new algorithm to calculate weighted flow-accumulation from a DEM by considering surface and underground stormwater infrastructure. *Environ. Model. Softw.* **2012**, *30*, 81–91. [CrossRef]

41. Taylor, K.E. Summarizing multiple aspects of model performance in a single diagram. *J. Geophys. Res.* **2001**, *106*, 7183–7192. [CrossRef]

42. Horton, R.E. Erosional development of streams and their drainage basins: Hydro-physical approach to quantitative morphology. *Geol. Soc. Am. Bull.* **1945**, *56*, 275–370. [CrossRef]

43. Strahler, A.N. Hypsometric (area-altitude) analysis of erosional topology. *Geol. Soc. Am. Bull.* **1952**, *63*, 1117–1142. [CrossRef]

44. Bai, R.; Li, T.J.; Huang, Y.F.; Li, J.Y.; Wang, G.Q.; Yin, D.Q. A hierarchical method for managing massive data of drainage networks extracted from high resolution DEM for large scale river basins. *Comput. Geosci.* **2015**, *85*, 234–247. [CrossRef]

45. Wohl, E.E. Hydrology and Discharge. In *Large Rivers: Geomorphology and Management*; Gupta, A., Ed.; John Wiley & Sons: Hoboken, NJ, USA, 2007.

46. Shi, H.Y.; Fu, X.D.; Chen, J.; Wang, G.Q.; Li, T.J. Spatial distribution of monthly potential evaporation over mountainous regions: Case of the Lhasa River basin, China. *Hydrol. Sci. J.* **2014**, *59*, 1856–1871. [CrossRef]

47. Conway, D.; Persechino, A.; Ardoin-Bardin, S.; Hamandawana, H.; Dieulin, C.; Mahe, G. Rainfall and water resources variability in sub-Saharan Africa during the twentieth century. *J. Hydrometeorol.* **2009**, *10*, 41–59. [CrossRef]

48. Barbarossa, V.; Huijbregtsa, M.A.J.; Hendriks, A.J.; Beusen, A.H.W.; Clavreul, J.; King, H.; Schipper, A.M. Developing and testing a global-scale regression model to quantify mean annual streamflow. *J. Hydrol.* **2017**, *544*, 479–487. [CrossRef]

49. Barbarossa, V.; Huijbregtsa, M.A.J.; Beusen, A.H.W.; Beck, H.E.; King, H.; Schipper, A.M. FLO1K, global maps of mean, maximum and minimum annual streamflow at 1 km resolution from 1960 through 2015. *Sci. Data* **2018**, *5*, 180052. [CrossRef] [PubMed]

50. Joyce, R.J.; Janowiak, J.E.; Arkin, P.A.; Xie, P.P. CMORPH: A method that produces global precipitation estimates from passive microwave and infrared data at high spatial and temporal resolution. *J. Hydrometeorol.* **2004**, *5*, 487–503. [CrossRef]

51. Huffman, G.J.; Adler, R.F.; Bolvin, D.T.; Gu, G.J.; Nelkin, E.J.; Bowman, K.P.; Hong, Y.; Stocker, E.F.; Wolff, D.B. The TRMM Multi-satellite Precipitation Analysis (TMPA): Quasi-global, multi-year, combined-sensor precipitation estimates at fine scales. *J. Hydrometeorol.* **2007**, *8*, 38–54. [CrossRef]

52. Allen, R.G.; Tasumi, M.; Trezza, R. Satellite-based energy balance for mapping evapotranspiration with internalized calibration (METRIC)-Model. *Irrig. Drain. Eng.* **2007**, *133*, 380–394. [CrossRef]

53. Oki, T.; Kanae, S. Global Hydrological Cycles and World Water Resources. *Science* **2006**, *313*, 1068. [CrossRef] [PubMed]

54. Wang, G.Q.; Fu, X.D.; Shi, H.Y.; Li, T.J. Watershed sediment dynamics and modeling: A watershed modeling system for Yellow River. Advances in Water Resources Engineering. In *Handbook of Environmental Engineering*; Yang, C.T., Wang, L.K., Eds.; Springer: Cham, Switzerland; Heidelberg, Germany; New York, NY, USA; Dordrecht, The Netherlands; London, UK, 2015; Volume 14, Chapter 1, pp. 1–40.

55. Barros, R.; Isidoro, D.; Aragüés, R. Long-term water balances in La Violada irrigation district (Spain): I. Sequential assessment and minimization of closing errors. *Agric. Water Manag.* **2011**, *102*, 35–45. [CrossRef]

56. Shi, H.Y.; Li, T.J.; Liu, R.H.; Chen, J.; Li, J.Y.; Zhang, A.; Wang, G.Q. A service-oriented architecture for ensemble flood forecast from numerical weather prediction. *J. Hydrol.* **2015**, *527*, 933–942. [CrossRef]

57. Shi, H.Y.; Li, T.J. Estimating hydrological parameters based on rainfall patterns in river basins with no long-term historical observations. *J. Hydrol.* **2017**, *553*, 651–661. [CrossRef]